EuroIntervention 2014;10:277-284

Evaluation of lesion and thermodynamic characteristics of Symplicity and EnligHTN renal denervation systems in a phantom renal artery model

Sara I. Al Raisi[1,2], MBBS; Jim Pouliopoulos[1,3], PhD; Michael T. Barry[1,3], BSc; John Swinnen[2,3], MBBS, FRACS; Aravinda Thiagalingam[1,3], MBBS, PhD; Stuart P. Thomas[1,3], MBBS, PhD; Gopal Sivagangabalan[1,3], MBBS, PhD; Clara Chow[1,4], MBBS, PhD; James Chong[1,3], MBBS, PhD; Eddy Kizana[1,3], MBBS, PhD; Pramesh Kovoor[1,3]*, MBBS, PhD

1. Department of Cardiology, Westmead Hospital, Sydney, NSW, Australia; 2. Department of Vascular Surgery, Westmead Hospital, Sydney, NSW, Australia; 3. University of Sydney, NSW, Australia; 4. The George Institute for International Health, Sydney, NSW, Australia

KEYWORDS

- renal disease
- risk factors
- safety

Abstract

Aims: Radiofrequency renal artery denervation has been used effectively to treat resistant hypertension. However, comparison of lesion and thermodynamic characteristics for different systems has not been previously described. We aimed to assess spatiotemporal lesion growth and ablation characteristics of Symplicity and EnligHTN systems.

Methods and results: A total of 39 ablations were performed in a phantom renal artery model using Symplicity (n=17) and EnligHTN (n=22) systems. The phantom model consisted of a hollowed gel block surrounding a thermochromic liquid crystal (TLC) film, exhibiting temperature sensitivity of 50-78°C. Flow was simulated using 37°C normal saline with impedance equal to blood. Radiofrequency ablations with each system were delivered with direct electrode tip contact to the TLC. Lesion size was interpreted from the TLC as the maximum dimensions of the 51°C isotherm. Mean lesion depth was 3.82 mm±0.04 versus 3.44 mm±0.03 ($p<0.001$) for Symplicity and EnligHTN, respectively. Mean width was 7.17 mm±0.08 versus 6.23 mm±0.07 ($p<0.001$), respectively. With EnligHTN, steady state temperature was achieved 20 sec earlier, and was 15°C higher than Symplicity.

Conclusions: In this phantom model, Symplicity formed larger lesions compared to EnligHTN with lower catheter-tip temperature. The clinical significance of our findings needs to be explored further.

Corresponding author: Cardiac Services, PO Box 533, Westmead Hospital, Cnr of Hawkesbury and Darcy Road, Sydney, NSW, 2145, Australia. E-mail: pramesh.kovoor@sydney.edu.au

SUBMITTED ON 06/01/2014 - 1st REVISION RECEIVED ON 23/03/2014 - 2nd REVISION RECEIVED ON 16/05/2014 - ACCEPTED ON 20/05/2014

DOI: 10.4244/EIJV10I2A46

Introduction

Refractory hypertension affects about 10-30% of hypertensive patients[1]. Renal artery denervation has resulted in a significant and sustained blood pressure reduction in patients with resistant hypertension as demonstrated by clinical trials[2,3]. The procedure aims to interrupt the neurohormonal impulses arising from the kidneys, which have been implicated in the pathogenesis of essential hypertension[4-7]. Nerves responsible for these signals lie within the adventitia of the renal artery with about 90% of nerve fibres occurring within 2 mm from the intimal surface[8]. Endovascular denervation of the renal arteries has been performed through different energy modalities, including radiofrequency, cryoablation, ultrasound, and chemical denervation[9-13]. At present, the two most widely utilised systems are the radiofrequency Symplicity™ (Medtronic, Minneapolis, MN, USA) and EnligHTN (St. Jude Medical, St. Paul, MN, USA) systems. Radiofrequency energy causes tissue destruction by means of thermal injury[14], when tissue temperature is raised above 45-50°C[15]. Both systems are optimised to operate with unique ablation settings summarised in **Table 1**.

Table 1. Clinical settings for the Symplicity and EnligHTN systems.

System parameters	Symplicity	EnligHTN
Monitoring	Temperature and impedance-based algorithm	Temperature-controlled algorithm
Number of electrodes	1	4
Maximal power (W)	8	6
Maximal temperature (°C)	70	75
Ablation duration (sec)	120	90

A predetermined algorithm is utilised for each system to ensure ablation safety. The goal is to achieve reasonably large lesions affecting the target nerves, whilst limiting the injury to the renal artery in order to minimise the risk of renal artery stenosis. It is therefore important to understand the basic biophysical properties for each system in relation to factors that may affect lesion formation. Assessment of the thermal characteristics of cardiac radiofrequency ablation using *in vivo* and *in vitro* models has been described previously[16,17]. Previous studies have demonstrated good correlation between radiofrequency ablation lesions performed in myocardium, and a Phytagel™ based myocardial phantom model incorporating a TLC film (LCR Hallcrest, Flintshire, UK)[17]. The study demonstrated the ability of TLC to map the dynamics of lesion formation, based on the 50°C isotherm, in high spatial and temporal resolution. Herein, we provide the first report to evaluate ablation characteristics for two renal denervation systems using a TLC phantom model of the human renal artery.

Editorial, see page 178

Methods

PHANTOM RENAL ARTERY MODEL

A renal artery model was prepared as per Chik[17]. Briefly, 1 gram of gel (Phytagel™; Sigma-Aldrich, St. Louis, MO, USA) was dissolved in a mixture of distilled water and normal saline at a pre-specified concentration (70% distilled water and 30% normal saline). The mix was then brought to a temperature of 90°C, and poured into a well once cooled down to 75°C. The gel well was immersed in a tank that pumped saline at a constant temperature (37°C). Impedance of saline used in the tank was matched to that of blood at 37°C. To mimic the renal artery with a comparable diameter and physiological blood flow rate in a human renal artery[18], specific modifications to the model were applied. In summary, this was achieved by pouring the gel around a 5 mm diameter metal rod holding a vertical TLC disc (colour bandwidth from 50-78°C) at the centre of the gel well. The rod was retrieved after gel cooling to form a hollowed tube in the centre of the gel simulating a renal artery lumen **(Figure 1)**. The diameter of the phantom renal artery was kept constant (5 mm) for all gel blocks used in the experiment. A flow meter was used to maintain the rate of saline pumped into the phantom renal artery at 500 ml/min.

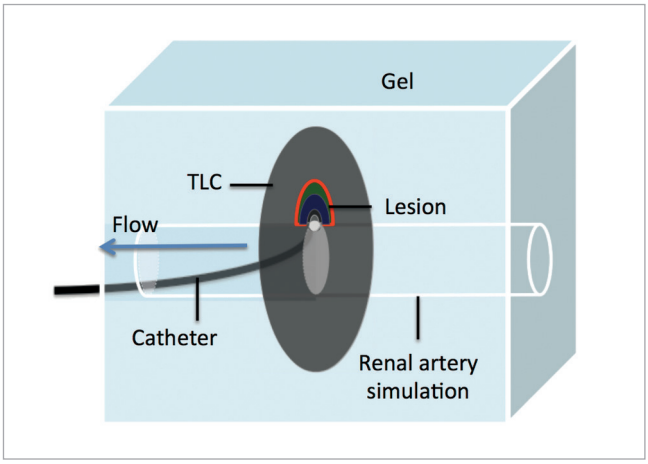

Figure 1. *Schematic diagram of radiofrequency ablation in a renal artery phantom model.*

RADIOFREQUENCY ABLATION ON TLC

An average of eight radiofrequency ablations per system were delivered on each gel block (n=3). A new TLC disc was used per gel block to avoid damage to the TLC by repeated heating. The order in which each system was tested was altered randomly with every new gel. To deliver radiofrequency ablations, the catheter (Symplicity or EnligHTN) was advanced through the phantom renal artery and positioned in plane with the TLC film. Contact was confirmed by direct visualisation, as the gel was transparent. Radiofrequency ablation was then applied to the gel using the recommended clinical parameters for each system as indicated in **Table 1**. In the case of EnligHTN, the small size basket was used to match the diameter of our phantom renal artery.

LESION MEASUREMENTS AND ANALYSIS

Photographs of the TLC colour gradient were taken at baseline and at 5 sec intervals during ablation using a digital camera (Canon EOS 5D Mark II; Canon Inc., Tokyo, Japan) and a light source (Canon

Speedlite 580EX; Canon Inc.). In-house software was used to analyse the pictures and measure lesion dimensions at several ablation intervals (initially every 5 sec, then every 10 sec) as described previously[17]. Lesion size was defined using the 51°C isotherm. Lesion depth was measured from the gel electrode surface to the isotherm of interest (51°C). Lesion width was defined as the maximal width of the 51°C isotherm parallel to the electrode gel surface **(Figure 2)**.

ELECTRODE SURFACE AREA IN CONTACT WITH GEL

For all ablations a cavity was created in the TLC and the gel to simulate endothelial tissue depression during electrode tip contact. The surface area in contact with the electrode was estimated to be about 50% of the total ablation electrode surface area for all energy applications. Measurements of electrode dimensions were carried out using a vernier scale **(Figure 3)**.

1. For Symplicity, total electrode surface area was calculated as follows:
   Total surface area (A_{TS})=Surface area 1 (A_1)+Surface area 2 (A_2)
   Given that r=0.62 mm and h=1.02 mm
   $A_1=4\,\pi\,r^2 / 2=2.42$ mm^2
   $A_2=2\,\pi\,r\,h=3.97$ mm^2, hence,
   $A_{TS}=6.39$ mm^2

Therefore, Symplicity electrode area in contact with gel=3.2 mm^2.

2. For EnligHTN, total surface area (A_{TE})=$2L\pi\sqrt{0.5(a^2+b^2)}$=3.7 mm^2, where L=0.97 mm, a=0.42, b=0.75 mm

Therefore, EnligHTN electrode area in contact with gel=1.85 mm^2.

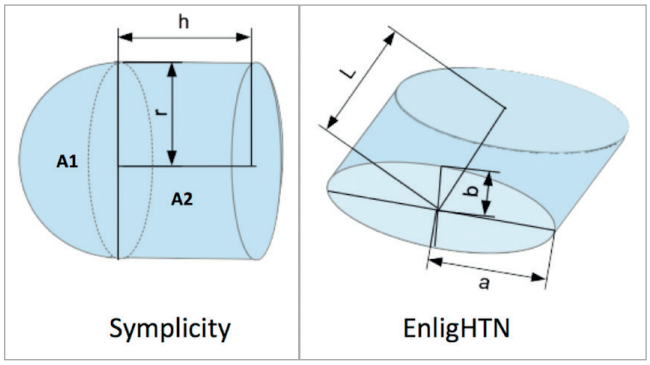

Figure 3. *Schematic diagram of Symplicity and EnligHTN electrode tip measurements.*

Statistical analysis

Based on preliminary data from gel 1 experiments, a total sample size of six ablations (three per catheter modality) was required to detect a mean difference of 0.66 mm for depth, and 1.54 mm for width with a power of 95% between each catheter modality when a=0.05 (two-tailed). As sufficient power was achieved to detect differences between modalities in the first experiment (gel 1), additional experimentation using multiple gels was performed to negate the effect of variation in the gel substrate, which may occur due to external factors (gel heating and solidification time). Mean depth and width for each system were determined using an unpaired

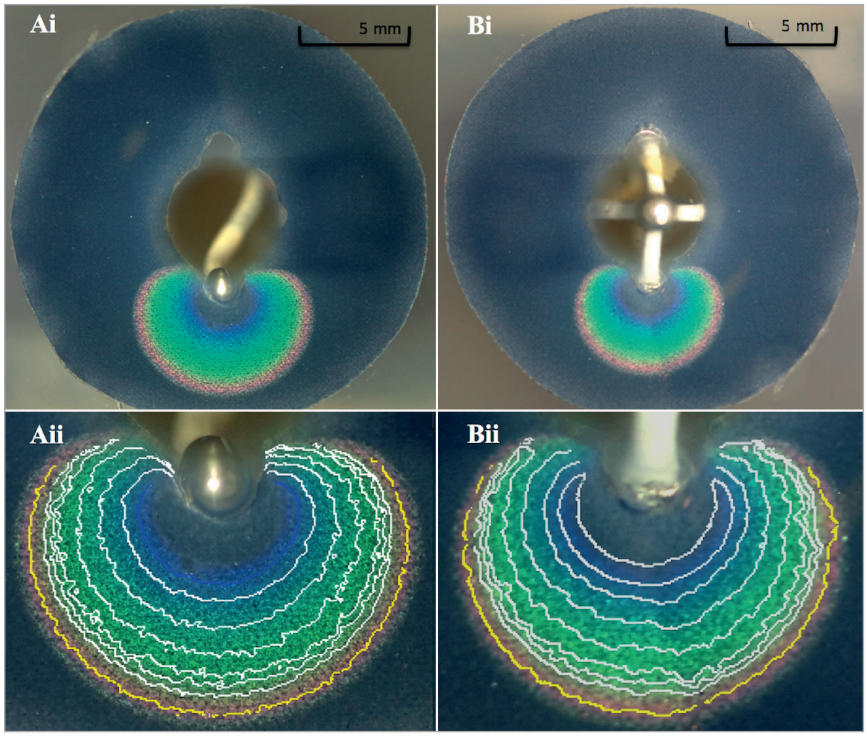

Figure 2. *Coronal image of gel with Symplicity (Ai) and EnligHTN (Bi) radiofrequency ablation of TLC film with related isotherm gradient at 120 sec and 90 sec, respectively, and their magnifications (Aii & Bii). The isotherm of interest (51°C) is highlighted in yellow (Aii & Bii).*

two-tailed Student's t-test. Each gel experiment for lesion dimensions (depth and width) was analysed using a two-way ANOVA. Pearson's correlation was used to assess the relationship between lesion dimensions (depth and width) with time, and power with time. Statistics were performed on GraphPad Prism 6.0 (GraphPad Software, San Diego, CA, USA). A linear mixed effects model was used to calculate the rate of temperature rise over time for the two systems. S-PLUS Version 8 was used to fit linear mixed effects models to the catheter temperature. In these models, ablation repetition and gel were considered as random factorial effects and time as a random continuous variable. Catheter type, time (continuous) and catheter by time interaction term were considered as fixed effects.

Results

A total of 52 ablations were performed on the phantom renal artery model, comprising 26 ablations for each system. A total of eight ablations using Symplicity and four ablations using EnligHTN were excluded from the analysis due to incorrect plane alignment between the catheter tip and TLC plate. Incorrect plane alignment refers to a catheter positioned inadequately on the TLC surface, but which could still be in contact with the gel. Therefore, the centre of the ablation zone (where maximal lesion dimension could be measured) occurs either behind or in front of the TLC, which will subsequently lead to underestimation of lesion dimensions. The exclusion rate for the Symplicity catheter was much higher because catheter positioning was technically more difficult with the Symplicity catheter compared to EnligHTN. Radiofrequency ablation parameters are summarised in **Table 2**.

LESION DIMENSION

Mean lesion depth was 3.82 mm±0.04 and 3.44 mm±0.03 ($p<0.001$) for Symplicity and EnligHTN, respectively. Mean width was 7.17 mm±0.08 versus 6.23 mm±0.07 ($p<0.001$), respectively **(Figure 4Ai, Figure 4Aii)**. Variability in lesion characteristics (range

Table 2. Parameters for Symplicity and EnligHTN ablations on the phantom model.

Ablation characteristics	Symplicity	EnligHTN	*p*
Number of ablations analysed	17	22	–
Mean maximal electrode temperature (°C)	55.11±1.04	68.91±0.94	<0.001
Mean baseline impedance (Ω)	199.9±1.12	216.2±1.28	<0.001
Mean baseline temperature (°C)	37.24±0.14	37.18±0.16	0.80
Mean power (W)	6.23±0.7	5.18±0.5	0.26
Electrode surface area in contact (mm^2)	3.2	1.85	–
Ablation duration (sec)	120	90	–

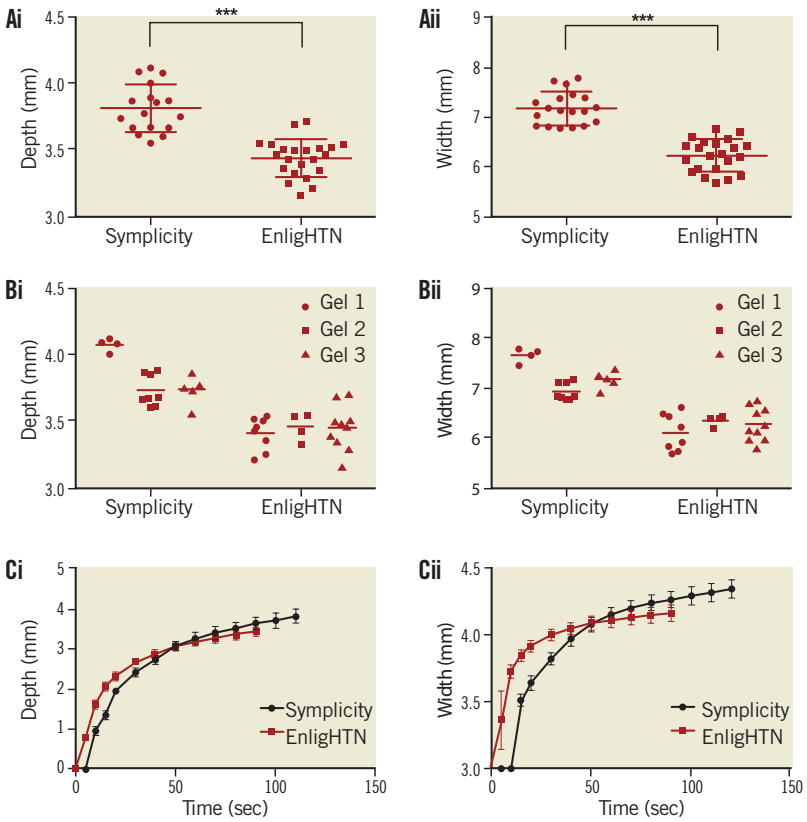

Figure 4. *Scatter plots comparing lesion depth (Ai) and width (Aii) for Symplicity and EnligHTN for all three gels combined and each gel separately (Bi, Bii). Graph of lesion growth, depth (Ci) and width (Cii), over duration of radiofrequency application with both systems.*

of width, and depth in mm) was observed between gels but, despite this, statistical significance between ablation systems was achieved **(Figure 4Bi, Figure 4Bii)**. This variability could be attributed to minor differences in the gel and TLC set-up, as well as electrode-TLC contact.

When analysed at 90 sec, there was no significant difference in lesion depth between the Symplicity and EnligHTN, with mean depth of 3.51 mm±0.04 versus 3.44 mm±0.03 (p=0.16). However, at 90 sec the difference in lesion width remained significant with mean width of 6.76 mm±0.07 versus 6.23 mm±0.07 (p<0.001) for Symplicity and EnligHTN, respectively. During Symplicity ablation, lesions continued to grow gradually over time, whereas lesion growth appeared to trend towards a plateau with EnligHTN at an earlier time point than Symplicity **(Figure 4Ci, Figure 4Cii)**.

ABLATION THERMODYNAMICS

Using EnligHTN, steady state temperature was achieved within 20-30 sec, while Symplicity took longer (50 sec) **(Figure 5A)**. This trend was consistent with the power output curve, whereby maximal power was reached within 10 sec for EnligHTN compared to a more gradual increase with Symplicity **(Figure 5B)**. This delay in heating with the Symplicity system may be due to an automated algorithm used to increase ablation safety. The maximal power output limit for each system was reached with all ablations. Within the first 20 sec of ablation, the rate of Symplicity electrode temperature rise was 0.2°C per sec (SE 0.065) faster than EnligHTN (p<0.0024). Additionally, EnligHTN had a higher electrode temperature at steady state 68°C compared to 55°C for Symplicity, p<0.001.

Discussion

Renal artery denervation is a promising treatment option for patients with resistant hypertension. However, a lot of questions remain unanswered regarding this treatment approach, as has been outlined recently[19]. One of the unknown factors is the safety and efficacy across different ablation systems and energy modalities. The present study is the first to compare ablation characteristics of two commercially available radiofrequency renal artery denervation systems directly using a phantom renal artery model. We found that Symplicity created lesions that were significantly deeper and wider than EnligHTN when duration of radiofrequency energy delivery was 120 sec and 90 sec, respectively, as recommended by the manufacturers. When ablation time was capped at 90 sec, lesion depths were similar between systems but remained significantly wider using Symplicity.

Thermal necrosis of tissue using radiofrequency energy occurs as a result of resistive and conductive heating[20]. During radiofrequency ablation resistive heating occurs within 1 mm of the myocardial-electrode interface, whereas deeper tissue heating results from slower thermal conduction which occurs in a radial pattern away from the resistive zone. Factors that lead to a larger volume of resistive heating or higher current density at the electrode tissue interface will similarly increase the temperature radial gradient area and subsequently lesion size[20]. These include ablation power, ablation duration, electrode surface area in contact with tissue, and ablation temperature.

In general, power increase leads to a greater current density at the electrode tissue interface. Therefore, lesion size is proportional to ablation power. An *in vivo* closed chest endocardial ablation study by Wittkampf demonstrated an increase in lesion size with higher power settings[21]. Similar results were obtained during *ex vivo* ablations of a bovine left ventricle under superfusate flow (1 L/min)[22]. The amount of power delivered to the target tissue is however affected by tissue impedance and power dissipation into the blood pool, which varies between different positions within one patient and also between different patients. Both Symplicity and EnligHTN systems operate at low power settings compared to cardiac radiofrequency ablation generators and are regulated by a catheter tip-temperature and impedance feedback mechanism. In our phantom model, mean power delivered during radiofrequency ablation was comparable for both systems. Hence, differences in lesion dimensions between the two systems cannot be explained by differences in power output.

Lesion growth rate for radiofrequency ablation follows a monoexponential function with a rapid initial phase occurring locally to the area of resistive heating. Thereafter, growth reaches a steady state without subsequent increase in lesion size[21,23]. A study that compared cardiac lesion size at two ablation time points (60 and 120 sec), utilising low ablation power

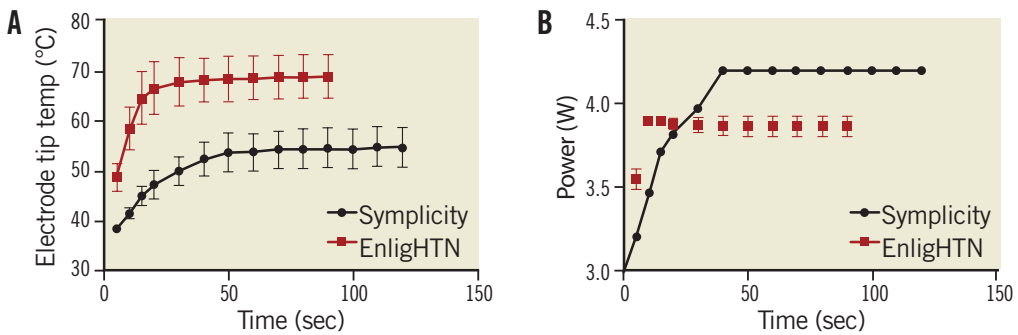

Figure 5. *Graph showing temperature change (A) and power output (B) over the duration of radiofrequency application for Symplicity and EnligHTN.*

ranging from 20-50 W and superfusate flow, showed that larger lesions occurred at 120 sec compared to 60 sec[22]. Based on that study, we postulate that the relatively longer ablation time applied using Symplicity was a significant factor in the observed increase in lesion size compared to EnligHTN. In support of this, neither system reached growth steady state, which is probably due to the high flow rate accounting for dissipation of power and reduction in power delivered to the tissue. This suggests that longer duration of ablation could potentially result in larger lesion size with both systems.

Lesion size is also affected by electrode tissue interface area. Haines described a linear relationship between electrode radius and lesion radius under constant electrode tissue interface temperature using a thermodynamic model. His model was validated using perfused and superfused canine right ventricular free wall[24]. Larger electrode radius formed bigger lesions when power density and tissue interface temperature remained constant. Nevertheless, higher overall power was required to maintain a similar power density. Additionally, lesion dimensions increase with increasing electrode length provided contact is adequate[25,26]. It has been demonstrated that increases in electrode tissue interface area and area exposed to convective cooling by blood are both responsible for increase in lesion size with larger electrodes[27]. Thus, the larger Symplicity electrode tissue interface area may have contributed to the difference in lesion size between the two catheters. Of note, the Symplicity system is based on a temperature and impedance algorithm, while the EnligHTN system has a temperature-controlled algorithm. The difference in system operation could also influence lesion size.

During temperature-controlled radiofrequency ablation, lesion size is directly proportional to electrode tissue interface temperature[20]. Temperature monitoring devices (thermocouple or thermistor) embedded within the ablation electrode monitor electrode tip temperature during radiofrequency ablation. However, a discrepancy between catheter tip temperature and tissue temperature can occur due to various factors including convective cooling by blood or irrigation. Whilst EnligHTN ablations reached higher electrode tip temperature compared to Symplicity for all ablations, Symplicity lesions were larger. This is probably due to the contribution of other factors discussed above affecting lesion size. Moreover, temperatures at the TLC electrode interface for all ablations were higher than those detectable by the TLC sheet (indicated by colour clearing, **Figure 2**), suggesting that the temperature measured by the electrode tip during renal artery ablation was lower than that of the electrode tissue interface. This difference was probably due to cooling of the electrode tip by high flow rate in the renal artery.

Thrombus formation and intimal disruption have been reported in a study using optical coherence tomography during renal artery denervation, more frequently with EnligHTN[28]. It is unclear if this is due to the higher temperature achieved during ablation and more rapid temperature increase with EnligHTN observed in our study.

Clinical implications

With numerous emerging technologies and catheter designs for renal artery denervation, it is critical to understand the basic biophysics of radiofrequency ablation for each device and the affect of that design on lesion formation. Moreover, identifying the unique characteristics of each renal denervation system is of pivotal importance in order to optimise ablation safety and efficacy. Each system needs to be evaluated further in clinical trials to establish its clinical safety and efficacy.

In the present study, adequate contact between the catheter tip and the TLC was confirmed by direct visualisation. However, in clinical practice this is difficult to establish and maintain, especially with the single electrode Symplicity catheter. This is important, as adequate electrode tissue contact is imperative for lesion formation[29]. In addition, despite the statistical difference in lesion size, it is difficult to anticipate the clinical significance of this finding.

Study limitations

The phantom renal artery used for our study does not replicate the heterogeneity of renal arterial layers, which have unique conduction properties and are also surrounded by fat. This may consequently affect the distribution of thermal injury. Nonetheless, the two systems were compared under an identical controlled environment with no confounding variables. This model also has the advantage of allowing the evaluation of temporal progression of lesions, which is difficult to assess *in vivo*. To allow for the comparison between the two systems, the flow rate and the renal artery diameter were kept constant; therefore, the effect of alteration in flow rate, arterial spasms and vessel wall oedema that can occur during the application of radiofrequency energy could not be simulated. In addition, EnligHTN lesions were more consistent in size compared to Symplicity lesions, as seen in **Figure 4B**. This could be as a result of variations in the electrode contact area with the gel-TLC surface, which were carefully placed but were more difficult to establish between the Symplicity experiments. Evaluation of collateral damage using the phantom model is not possible; however, a preclinical safety trial conducted with the Symplicity system reported no collateral damage to kidneys or nearby structures[30]. Finally, the TLC film used in the phantom had a colour change sensitivity range between 50-78°C; therefore, we were unable to detect temperatures beyond this range.

Conclusion

Lesion size was larger for the Symplicity renal artery denervation system compared to EnligHTN when radiofrequency ablation was performed on a phantom renal artery model. The difference in lesion size was more pronounced for lesion width, with a smaller difference in lesion depth. This was achieved with a gradual increase in temperature and lower electrode tip temperature at steady state with the Symplicity system. It is likely that the larger electrode surface area and longer ablation duration with Symplicity could have accounted for the difference in lesion size.

Impact on daily practice

One important criterion for successful renal artery denervation is the delivery of safe and effective ablation lesions. Currently, different systems are being used to deliver these ablations in patients with resistant hypertension. Understanding the biophysical properties of the systems and the differences in lesions formed is essential to improve the techniques and clinical outcome. The renal artery phantom model described here provided a platform to identify lesion properties from two different systems under specific conditions. This model can be applied to available and future renal denervation systems, thereby providing a preclinical simulation that would objectively inform the clinical parameters for the lesions created.

Conflict of interest statement

The authors have no conflicts of interest to declare.

References

1. Calhoun DA, Jones D, Textor S, Goff DC, Murphy TP, Toto RD, White A, Cushman WC, White W, Sica D, Ferdinand K, Giles TD, Falkner B, Carey RM; American Heart Association Professional Education Committee. Resistant hypertension: diagnosis, evaluation, and treatment: a scientific statement from the American Heart Association Professional Education Committee of the Council for High Blood Pressure Research. *Circulation*. 2008;117:e510-26.

2. Krum H, Schlaich M, Whitbourn R, Sobotka PA, Sadowski J, Bartus K, Kapelak B, Walton A, Sievert H, Thambar S, Abraham WT, Esler M. Catheter-based renal sympathetic denervation for resistant hypertension: a multicentre safety and proof-of-principle cohort study. *Lancet.* 2009;373:1275-81.

3. Esler MD, Krum H, Schlaich M, Schmieder RE, Bohm M, Sobotka PA. Renal sympathetic denervation for treatment of drug-resistant hypertension: one-year results from the Symplicity HTN-2 randomized, controlled trial. *Circulation*. 2012;126:2976-82.

4. DiBona GF. Physiology in perspective: The Wisdom of the Body. Neural control of the kidney. *Am J Physiol Regul Integr Comp Physiol.* 2005;289:R633-41.

5. Esler M, Jennings G, Lambert G. Noradrenaline release and the pathophysiology of primary human hypertension. *Am J Hypertens.* 1989;2:140S-146S.

6. Campese VM, Kogosov E, Koss M. Renal afferent denervation prevents the progression of renal disease in the renal ablation model of chronic renal failure in the rat. *Am J Kidney Dis.* 1995;2:861-5.

7. Katholi RE, Winternitz SR, Oparil S. Decrease in peripheral sympathetic nervous system activity following renal denervation or unclipping in the one-kidney one-clip Goldblatt hypertensive rat. *J Clin Invest.* 1982;69:55-62.

8. Atherton DS, Deep NL, Mendelsohn FO. Micro-anatomy of the renal sympathetic nervous system: a human postmortem histologic study. *Clin Anat.* 2012;25:628-33.

9. Honton B, Pathak A, Sauguet A, Fajadet J. First report of transradial renal denervation with the dedicated radiofrequency Iberis catheter. *EuroIntervention.* 2014;9:1385-8.

10. Fischell TA, Vega F, Raju N, Johnson ET, Kent DJ, Ragland RR, Fischell DR, Almany SL, Ghazarossian VE. Ethanol-mediated perivascular renal sympathetic denervation: preclinical validation of safety and efficacy in a porcine model. *EuroIntervention.* 2013;9:140-7.

11. Heuser RR, Mhatre AU, Buelna TJ, Berci WL, Hubbard BS. A novel non-vascular system to treat resistant hypertension. *EuroIntervention.* 2013;9:135-9.

12. Ormiston JA, Watson T, van Pelt N, Stewart R, Stewart JT, White JM, Doughty RN, Stewart F, Macdonald R, Webster MW. Renal denervation for resistant hypertension using an irrigated radiofrequency balloon: 12-month results from the Renal Hypertension Ablation System (RHAS) trial. *EuroIntervention.* 2013;9:70-4.

13. Mabin T, Sapoval M, Cabane V, Stemmett J, Iyer M. First experience with endovascular ultrasound renal denervation for the treatment of resistant hypertension. *EuroIntervention.* 2012;8:57-61.

14. Erez A, Shitzer A. Controlled destruction and temperature distributions in biological tissues subjected to monoactive electrocoagulation. *J Biomech Eng.* 1980;102:42-9.

15. Cosman ER Jr, Cosman ER Sr. Electric and thermal field effects in tissue around radiofrequency electrodes. *Pain Med.* 2005;6:405-24.

16. Nakagawa H, Yamanashi WS, Pitha JV, Arruda M, Wang X, Ohtomo K, Beckman KJ, McClelland JH, Lazzara R, Jackman WM. Comparison of in vivo tissue temperature profile and lesion geometry for radiofrequency ablation with a saline-irrigated electrode versus temperature control in a canine thigh muscle preparation. *Circulation*. 1995;91:2264-73.

17. Chik WW, Barry MA, Thavapalachandran S, Midekin C, Pouliopoulos J, Lim TW, Sivagangabalan G, Thomas SP, Ross DL, McEwan AL, Kovoor P, Thiagalingam A. High spatial resolution thermal mapping of radiofrequency ablation lesions using a novel thermochromic liquid crystal myocardial phantom. *J Cardiovasc Electrophysiol.* 2013;24:1278-86.

18. Wolf RL, King BF, Torres VE, Wilson DM, Ehman RL. Measurement of normal renal artery blood flow: cine phase-contrast MR imaging vs clearance of p-aminohippurate. *AJR Am J Roentgenol.* 1993;161:995-1002.

19. Tsioufis C, Mahfoud F, Mancia G, Redon J, Damascelli B, Zeller T, Schmieder RE. What the interventionalist should know about renal denervation in hypertensive patients: a position paper by the ESH WG on the interventional treatment of hypertension. *EuroIntervention.* 2014;9:1027-35.

20. Nath S, DiMarco JP, Haines DE. Basic aspects of radiofrequency catheter ablation. *J Cardiovasc Electrophysiol.* 1994;5:863-76.

21. Wittkampf FH, Hauer RN, Robles de Medina EO. Control of radiofrequency lesion size by power regulation. *Circulation*. 1989;80:962-8.

22. Guy DJ, Boyd A, Thomas SP, Ross DL. Increasing power versus duration for radiofrequency ablation with a high superfusate

flow: implications for pulmonary vein ablation? *Pacing Clin Electrophysiol.* 2003;26:1379-85.

23. Haines DE. Determinants of lesion size during radiofrequency catheter ablation: the role of electrode-tissue contact pressure and duration of energy delivery. *J Cardiovasc Electrophysiol.* 1991;2:509-15.

24. Haines DE, Watson DD, Verow AF. Electrode radius predicts lesion radius during radiofrequency energy heating. Validation of a proposed thermodynamic model. *Circ Res.* 1990;67:124-9.

25. Langberg JJ, Gallagher M, Strickberger SA, Amirana O. Temperature-guided radiofrequency catheter ablation with very large distal electrodes. *Circulation*. 1993;88:245-9.

26. Kovoor P, Daly M, Campbell C, Dewsnap B, Eipper V, Uther J, Ross D. Intramural radiofrequency ablation. *Pacing Clin Electrophysiol.* 2004;27:719-25.

27. Otomo K, Yamanashi WS, Tondo C, Antz M, Bussey J, Pitha JV, Arruda M, Nakagawa H, Wittkampf FH, Lazzara R, Jackman WM. Why a large tip electrode makes a deeper radiofrequency lesion: effects of increase in electrode cooling and electrode-tissue interface area. *J Cardiovasc Electrophysiol.* 1998;9:47-54.

28. Templin C, Jaguszewski M, Ghadri JR, Sudano I, Gaehwiler R, Hellermann JP, Schoenenberger-Berzins R, Landmesser U, Erne P, Noll G, Lüscher TF. Vascular lesions induced by renal nerve ablation as assessed by optical coherence tomography: pre- and post-procedural comparison with the Simplicity catheter system and the EnligHTN multi-electrode renal denervation catheter. *Eur Heart J.* 2013;34:2141-8, 2148b.

29. Haines DE, Watson DD. Tissue heating during radiofrequency catheter ablation: a thermodynamic model and observations in isolated perfused and superfused canine right ventricular free wall. *Pacing Clin Electrophysiol.* 1989;12:962-76.

30. Rippy MK, Zarins D, Barman NC, Wu A, Duncan KL, Zarins CK. Catheter-based renal sympathetic denervation: chronic preclinical evidence for renal artery safety. *Clin Res Cardiol.* 2011;100:1095-101.